Beata Niezgoda-Żelasko (bniezgoda@mech.pk.edu.pl)

Institute of Thermal and Process Engineering, Faculty of Mechanics, Cracow University of Technology

Enhancement of the boiling process of refrigerants with high temperature glide and low GWP

Intensyfikacja procesu wrzenia czynników chłodniczych o dużym poślizgu temperaturowym i niskim GWP

Abstract

The paper presents the results of experimental studies of the enhancement of the boiling process of a zeotropic agent with high temperature glide inside tubes at a low heat flux density. It discusses the effect of three types of inserts on the heat transfer process and the flow resistances during boiling of R407C in vertical tubes. The experimental studies covered measurements of heat transfer coefficient values, flow resistance values and thermal efficiency in the measurement section.

Keywords: boiling, heat transfer enhancement inserts, heat transfer coefficients, flow resistances

Sreszczenie

Przedmiotem prezentowanej publikacji są wyniki badań eksperymentalnych intensyfikacji procesu wrzenia wewnątrz rur czynnika zeotropowego z dużym poślizgiem temperaturowym w warunkach niskich gęstości strumieni ciepła. W ramach pracy omówiono wpływ zastosowania trzech rodzajów wkładek na proces wymiany ciepła czynnika R407C i opory przepływu podczas wrzenia w rurach pionowych. Wyniki badań doświadczalnych obejmują pomiary wartości współczynników przejmowania ciepła, oporów przepływu oraz wydajności cieplnej uzyskiwanej w odcinku pomiarowym.

Słowa kluczowe: wrzenie, wkładki intensyfikujące wymianę ciepła, współczynniki przejmowania ciepła, opory przepływu

Nomenclature

A_w	–	inner tube surface area (copper tube), (m²)
d	–	diameter, (m)
d_p	–	outer coil diameter, diameter of the full insert, (m)
d_s	–	diameter of the spring rod, spring wound around a full insert, (m)
$\dot{G}$	–	refrigerant mass flux density, (kg/(m²s))
h	–	coil pitch, (m)
i	–	specific enthalpy, (J/kg)
$\dot{m}$	–	mass flux, (kg/s)
p	–	pressure, (Pa)
r	–	specific evaporation heat, (J/kg)
$\dot{q}$	–	heat flux density, (W/m²)
$\dot{Q}$	–	thermal efficiency, (W)
T	–	temperature, (°C)
T	–	temperature of the outer, inner tube wall, (°C)
V	–	volume of refrigerant in a tube with an insert, (m³)
x	–	vapour quality, (kg/kg)
X_{tt}	–	Lockhart-Martinelli parameter,

$\Delta T = \bar{T}_{walli} - \bar{T}_R$ – temperature difference in the definition of the heat transfer coefficient for the refrigerant, (K)

a	–	heat transfer coefficient, (W/(m²K))
l	–	heat conduction coefficient, (W/(mK))
g,l	–	gas phase, liquid phase
in,out	–	inlet, outlet
o	–	concerns the evaporation process in the test section
pt	–	plain tube
R	–	refrigerant (or water)
s	–	saturation state
sc, sv	–	subcooling, superheating
w1, w2	–	water cooling the condenser, water cooling the subcooler

1. Introduction

The use of refrigerants based on saturated and unsaturated hydrocarbons is motivated not only by their thermodynamic properties, but also by the environmental impact restrictions. As stated in [1], the use of HFCs with a GWP equal to or greater than 2500 will become prohibited after 2020 and the cap on GWP$_{gr}$ will be reduced to just 150 after 2022. Such restrictions are set to push a range of refrigerants, which are now commonly used in air-cooling and air-conditioning technology (such as R404A, R507, R410A) out of the market. The available replacements are either inflammable and explosive (e.g. R32, R290, R1234yF) or they have a

relatively high temperature glide (e.g. R407C, R449, Opteon XL40). A temperature glide in the boiling process translates into lower heat exchanger thermal efficiency.

This article discusses the results of experimental research into the enhancement of the tube boiling process of high-temperature-glide refrigerants at low heat flux densities. The author has focused on the impact of three types of inserts on the heat transfer process and flow resistances during vertical tube boiling. The results of the experimental research for various mass and heat flux density values have been discussed for R407C. The research covers the measurements of the values of heat transfer coefficients, flow resistances and thermal efficiency in the measurement section.

In recent years, tubes with micro-fins or specially structured heat transfer surfaces have been analysed by researchers with particular interest. A detailed review of publications discussing the boiling process on extended surfaces has been included in [2]. Ribatski and Thome [2] presented the results of their analyses of the boiling process of R134a outside several types of industrial finned tubes, i.e. High Flux, Gewa-B and Turbo-CSL (d_i=19.5 mm). The obtained heat transfer coefficient enhancement ratios varied from 1.8 to 21.9, depending on the tube type. Ribatski and Thome note that the greater the heat flux density, the less profitable it is to augment the heat transfer surface.

The boiling process inside horizontal tubes with micro-fins was discussed in [3-8]. The effect of the shape of the horizontal tube (circular cross-section w/h=1 and ellipsoidal cross-sections w/h=2, w/h=4) on heat transfer coefficients and flow resistance values of R410A was examined by Kim et al. [9].

Papers [10, 11] look at the effect of a spiral aluminium tape inserted into a tube on boiling heat transfer coefficients and two-phase flow resistances. Yun et al [12] presented the results of their analyses of the boiling process of nitrogen in horizontal tubes with a diameter d_i=10.6 mm with wire coil inserts with a coil diameter d_p=10 mm, wire thickness d_s=1.5; 2; 2.5 mm and coil pitch h=18.4; 27.6 and 36.8 mm.

2. 2. Description of the test stand and methods

The test stand used to study the boiling process inside vertical tubes with inner diameter d_i=0.021 m consisted of two bimetallic tubes with the height L=2 m in an in-line arrangement (Fig. 1). The inner tube was made of copper and had the inner and outer diameters d_i and d_o. The outer one was an aluminium tube with diameters d_o and d_{o1}. There were eight longitudinal aluminium fins on the outer surface of the tube on the air-side. The air-side heat transfer surface enhancement ratio was 16 [13]. The experimental results presented here were obtained during laboratory tests, which reflected the actual operating conditions of natural convection heat pump evaporators.

The test section (ET) made part of the evaporator system of a cooling device. The evaporator consisted of a preheater (Heat1), the test section (ET) and a superheater (Heat2). Heat was supplied to the preheater and the superheater by electric heaters, whose power was measured using wattmeters LW-1 ($\dot{Q}_{Heat1}$, $\dot{Q}_{Heat2}$). External air was the source of heat for the studied
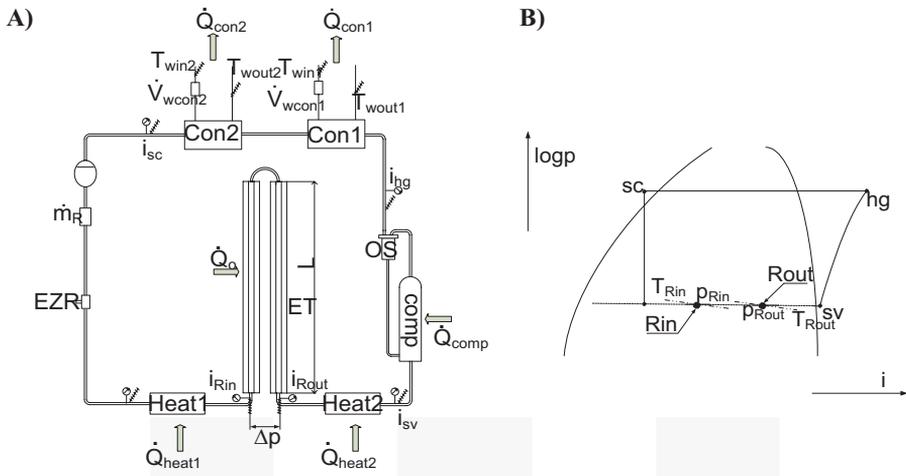
Fig. 1. A) An outline of the measurement stand: Heat1-preheater, ET-measurement section, Heat2-superheater, comp- compressor, con1- condenser, os- oil separator, con2- aftercooler, EZR-electronic expansion valve; B) Characteristic points of the cooling system on the logp-i graph

vertical tubes. A Copeland spiral compressor was another element of the cooling system. It was also fitted with an oil separator manufactured by GAR. Wattmeters were used to measure the power of the compressor's engine $\dot{Q}_{comp}$. The condensation section of the system consisted of a condenser (Con1) and a water-cooled subcooler (Con2). The refrigerant was channelled into the evaporator through an electronic expansion valve (EZR) with a specific aperture degree corresponding to the assumed refrigerant mass flux density ($\dot{G}$) and evaporation pressure (p_R). Each characteristic point of the cooling system was identified by measuring the temperature (Hart Scientific PT100(7013) resistance thermometer) and pressure (Vegabar 17 pressure transducer) of the refrigerant (compressor suction, discharge, inlet to the electronic expansion valve and a point downstream of the electronic expansion valve, Fig. 1b).

In addition, the parameters of the refrigerant (temperature T_R and pressure p_R) were measured at the inlet and at the outlet of the test section. Temperature sensors measuring the temperature of the refrigerant within the test section were installed in special measurement sleeves located on the supply and return elbows of the test section. The measurement sensor length of 152 mm enabled actual temperature measurements to be taken 132 mm from the elbow. In addition, the outside temperature of the heat transfer surface (T_{wallo}) was measured at the inlet and outlet of the test section, ca. 0.3 m from the elbow [13]. A refrigerant mass flow meter DI6-Mass6000 was installed on the liquid pipe in the cooling system. All the supply pipes of the cooling system, as well as the preheater and the superheater, were insulated with rubber insulation with a heat conductivity coefficient of 0.034 W/(mK) and a thickness of 19 mm. The enthalpy value of the refrigerant at the characteristic points of the system and the physical properties (as a function of the mean value of evaporation pressure $\bar{p}_R$) of the refrigerants were calculated using RefproP.exe [14].

The total heat flux received at the evaporator, which is the sum of the thermal efficiency of the pre-heater $\dot{Q}_{Heat1}$, the test section $\dot{Q}_{o}$ and the super-heater $\dot{Q}_{Heat2}$, may be calculated on the basis of the heat balance equation on the refrigerant side:

$$\dot{Q}_{evap} = \dot{Q}_{Heat1} + \dot{Q}_{o} + \dot{Q}_{Heat2} = \dot{m}_{R}\left(i_{sv} - i_{sc}\right) \tag{1}$$

Equation (1) was used to calculate the heat flux supplied to the evaporator's tubes.

$$\dot{Q}_{o} = \dot{m}_{R}\left(i_{sv} - i_{sc}\right) - \left(\dot{Q}_{Heat1} + \dot{Q}_{Heat2}\right) \tag{2}$$

For R407C, the measurement of pressure and temperature at the inlet and outlet of the test section (Fig.1), as well as the Refprop software, made it possible to determine vapour quality x_{Rin}, x_{Rout} in the wet vapour area.

The mean vapour quality was calculated as the arithmetical mean of vapour quality at the inlet and outlet of the test section:

$$x_{m} = 0.5\left(x_{Rin} + x_{Rout}\right) \tag{3}$$

The heat transfer coefficient for the boiling refrigerant was calculated on the basis of equation (4), where the temperature of the inner tube wall was determined using formulas (5-6). The mean temperature of the refrigerant was calculated as the mean arithmetical temperature of the refrigerant at the inlet and outlet of the test section.

$$\alpha_{R} = \frac{\dot{Q}_{o}}{A_{w} \cdot \left(\overline{T}_{walli} - \overline{T}_{R}\right)} \tag{4}$$

$$\overline{T}_{walli} = \overline{T}_{wallo} - \frac{\dot{Q}_{o}}{A_{w}}R \tag{5}$$

$$\dot{Q}_{evap} = \dot{Q}_{Heat1} + \dot{Q}_{o} + \dot{Q}_{Heat2} = \dot{m}_{R}\left(i_{sv} - i_{sc}\right) \tag{6}$$

Equation (6) stands for the conductivity resistance of a bimetallic tube and results from the formulation of a heat conductivity equation for a cylindrical multi-layer partition.

The study looked at refrigerants, heat and mass flux densities and evaporation temperature as listed in Table 1.

Table 1. Scope of research into the boiling process inside vertical tubes

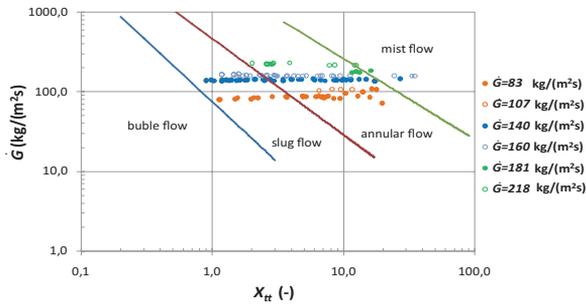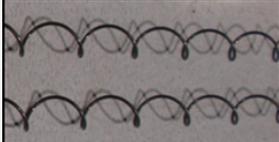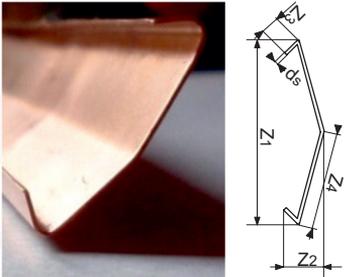| $\dot{q}\left(\text{W/m}^2\right)$	$\dot{G}\left(\text{kg/(m}^2\text{s)}\right)$	T_R (°C)	x_m (-)
$5000 \leq \dot{q} \leq 6000$ $9000 \leq \dot{q} \leq 11000$	$\dot{G} = 83$; 140; 160; 218	T_R=-20; -10; -7.5; 1.05	

Fig. 2.   Flow structures analysed during the boiling of R407C in vertical tubes, according to data shown in Table 1 and Fair's model [15]

Boiling was analysed in the areas corresponding to slug, annular and bubble flow structures [15] (Fig. 2). Three types of heat transfer enhancing elements were analysed (Table 2): an insert increasing the refrigerant flow velocity (a full insert, marked as WP, consisting of a brass core with a rod wound around it), a flow-turbulising coil spring (SP) and an insert, which turbulised the flow and increased the heat transfer surface (marked as Fin). The mean temperature of the refrigerant at the inlet and outlet of the test section – T_{Rin}, T_{Rout} – was measured by means of highly sensitive Pt100(7013) resistance sensors with

Table 2.   List of the studied heat transfer enhancing inserts

Full insert -WP	Spring-SP	Fin
$d_p = 0.01$ m, $d_s = 0.0014$ m, $h = 0.037$ m	$d_p = 0.0195$ m $d_s = 0.002$ m, $h = 0.043$ m	$Z_1 = 0.0212$ m $Z_2 = 0.0057$ m $Z_3 = 0.0035$ m $Z_4 = 0.00105$ m $d_s = 0.0006$ m

large overall dimensions (the diameter of the sensor mantle measured about 5 mm, active length - a minimum of 0.02m). The temperature of the wall T_{wall} was measured by means of Pt100(5622-05) (Hart Scientific resistance thermometer) sensors (diameter of the sensor mantle – 0.5 mm, minimum active length – 0.01m). In order to ensure high measurement accuracy for the temperature difference, the sensors were calibrated for the entire expected temperature range. Calibration was done by means of precision sensors (Pt100(7013))

directly at the measuring stand before each measurement series, using a Quartz-35 calibration furnace. This highly precise system for measuring temperature difference (of the tube wall and the medium flowing inside the tube) is as accurate as the Pt100(7013) sensors. The classical system with thermocouples, used for this kind of measurements, is by a grade less accurate.

The factor, which resulted in an error of determination of heat transfer coefficients, was the accuracy of determination of the heat flux transferred in the test section, which did not exceed 50W. For the maximum errors of determination of the direct and indirect values (Table 3), the calculated relative errors of the measured heat transfer coefficients have been shown in Table 3.

Table 3. Systemic uncertainties of intermediate values and mean relative errors of the heat transfer coefficients

Value	$\delta(\dot{Q})$ W	$\delta(DT)$ K	$\delta(A)$ m²
$\delta(\%)$	50	0,038	$1,2*10^{-3}$
Insert	SP	WP	Fin
$\Delta\alpha_R / \alpha_R \%$	12,4	13,3	10,9

3. Heat transfer and flow resistance coefficients - results of experimental studies

The test results indicate that when all the analysed types of inserts are considered, the highest heat transfer coefficients are recorded for the coil spring insert (SP). The WP insert turns out to be more effective with R407C (Fig. 3) and at lower refrigerant mass flux densities (Fig. 3a,c).

The most limited increase in heat transfer coefficient values was observed for the Fin insert, especially at low mass stream densities (Fig. 3a,c). Each insert works differently and hence the various effect of the mass flux density, temperature glide and heat flux density on the increase of heat transfer coefficients. As shown in Figure 3, SP inserts improved the heat transfer coefficient values in the entire studied vapour quality range. Indeed, a significant part of the tests focused on the convective boiling area with slug flow and annular flow patterns (Fig. 2, Fair-Thome model, [15]). A spring insert with a properly adjusted coil diameter causes greater flow turbulisation near the tube wall (e.g. in the liquid layer in annular flow), thus enhancing the convective heat transfer process characteristic of slug and annual flow.

The rod in the spring insert disturbs the flow and promotes the mixing of the fluid. WP inserts were used to increase the flow velocity of the refrigerant and break apart vapour bubbles, especially in the slug flow area. In addition, the use of a copper rod spirally wound around a brass core changed the refrigerant velocity profile by shifting its maximum velocity values towards the inner tube wall to achieve more turbulent flow in the boundary layer.

As it was to be expected, the WP insert generated the greatest flow resistances (Fig. 4). A drop in pressure is accompanied by a drop in boiling temperature and a greater difference in temperatures between the heat transferring media (in this case the air and the refrigerant). Lower boiling temperature corresponds to lower values of heat transfer coefficients.
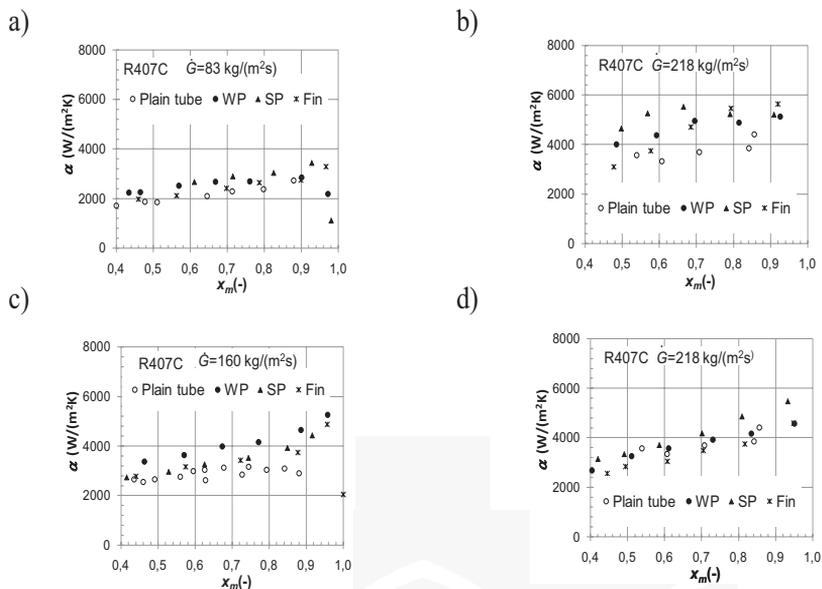
Fig. 3. Heat transfer coefficients measured for various types of inserts: a) $\dot{q} \approx 6$ kW/m², $\dot{G} = 83$ kg/(m²s), p_R=0,241 MPa; b) $\dot{q} \approx 6$ kW/m², $\dot{G} = 218$ kg/(m²s), p_R=0,526 MPa; c) $\dot{q} \approx 11$ kW/m², $\dot{G} = 83$ kg/(m²s), p_R=0,241 MPa; d) $\dot{q} \approx 9$ kW/m², $\dot{G} = 218$ kg/(m²s), p_R=0,526 MPa
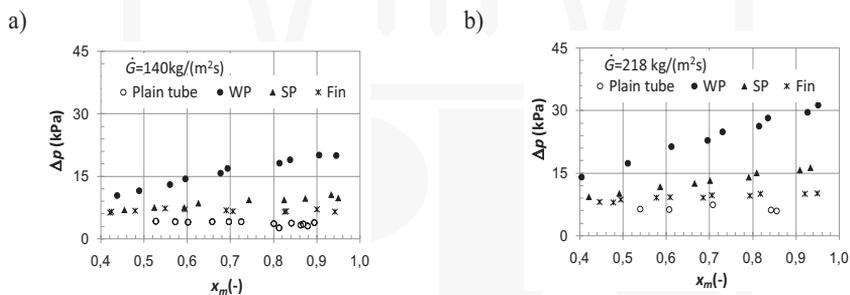

Fig. 4. Comparison of flow resistances in plain tubes and in tubes with heat transfer enhancing inserts:: a) $\dot{G} = 140$ kg/(m²s),, p_R=0,347 MPa; b) $\dot{G} = 218$ kg/(m²s),, p_R=0,526 MPa;

For high mass flux densities (Fig. 4b), the flow resistances of the insert increase significantly if a WP insert is used, and therefore, the insert only enhances the heat transfer process to a limited extent. In turn, for low mass flux densities, an increase in the flow velocity improves the convection boiling component with no clear decrease in the heat transfer coefficients caused by a drop in boiling temperature. In the case of refrigerants with significant temperature glide (R407C), a drop in refrigerant pressure is accompanied by the stabilisation of boiling temperature. Two opposing phenomena occur in this case: a decrease in the value of the heat transfer coefficient as a result of a greater difference in temperatures $\Delta T = \bar{T}_{walli} - \bar{T}_R$ (Fig. 3d, Fig.5b curve 2) and an increase in the thermal efficiency of the exchanger resulting from a

greater temperature difference between the cooling and the cooled medium (Fig. 5a, curve 1). For lower refrigerant mass flux density values (e.g. $\dot{G}$ =83 kg/(m²s) Fig. 5b), no such significant temperature differences $\Delta T = \bar{T}_{wall} - \bar{T}_R$ were observed for particular inserts as in the case of mass flux density $\dot{G}$ =218 kg/(m²s) (Fig. 5b).

The effectiveness of heat transfer through a finned surface depends both on the heat transfer coefficient and on the efficiency of the fin itself. In the experimental studies presented here for a Fin insert, the determined heat transfer coefficients take into consideration the impact of the fin efficiency on the heat transfer process. A decrease in the fin efficiency
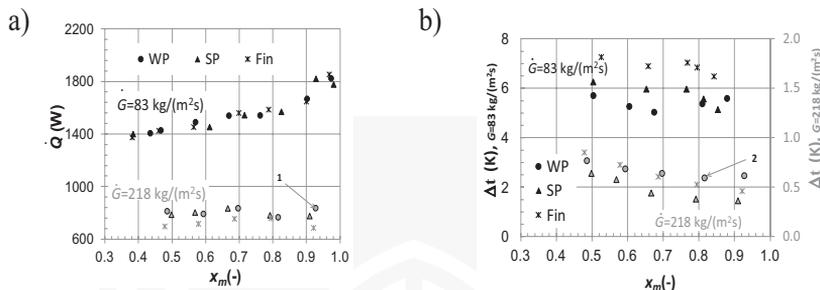

Fig. 5.   Measurement results for R407C: a) $\dot{Q}(x_m)$, $\dot{G} = 83$ kg/(m²s), $\dot{q} \approx 11000$ W/m²;

$\dot{G} = 218$ kg/(m²s), $\dot{q} \approx 6000$ Wm⁻²;

a) D$T=T_w$-T_R, $\dot{G} = 83$ kg/(m²s), $\dot{q} \approx 11000$ W/m²; b) D$T=T_w$-T_R, $\dot{G} = 218$ kg/(m²s)

resulting from an increase in the heat transfer coefficient may, however, be compensated by a sufficiently high value of the heat transfer coefficient. This applies to the analysed Fin insert. An experimentally determined heat transfer coefficient for a tube with a Fin insert is higher for higher flow velocity (resulting from an increase in the mass flux density of the refrigerant) and greater turbulence, which is a consequence of the presence of the insert and its geometrical shape. The shape of the insert where it is in contact with the inner tube surface leads to the development of areas where the flowing refrigerant is slowed down, especially if the mass flux density is low, and where vapour bubbles may be "retained". Low efficiency of the fin (due to its height and thickness), as well as low values of the heat transfer coefficient, make the heat flux transferred from the tube wall low, and therefore, the measured heat transfer coefficients are also low (Fig. 3a,c). As the mass flux density rises, the occurrence of "dead zones" in areas where the fin is in contact with the tube wall is minimised, and the measured values of heat transfer coefficients increase despite the fact that fin efficiency drops (Fig. 3b,d).

The heat transfer coefficient increase ratios (α/a_{pt}) presented in figure 6 tend to increase slightly for all insert types along with an increase in vapour quality within the range of $0.5<x_m<0.9$ (in the annular flow area), reaching a maximum value within the vapour quality range of $0.8<x_m<0.9$. A sharp decrease in the indicator's value is detectable in the mist flow area (α/a_{pt}).

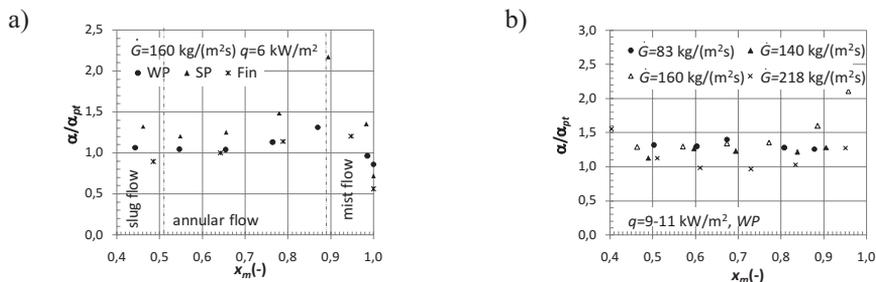The averaged values of the heat transfer coefficient increase ratios $\overline{(\alpha/\alpha_{pt})}(x)$ and flow

a)

b)

Fig. 6. Heat transfer coefficient increase indicators (α/a_{pt}): a) $\dot{q} \approx 11$ kW/m², $\dot{G} = 140$ kg/(m²s); b) WP insert, refrigerant , $\dot{q} \approx 9-11$ kW/m²

resistance ratios for the completed measurements have been listed in Table 4.

Table 4. Averaged values of the heat transfer coefficient and flow resistance increase ratios

Insert	$5000 \leq \dot{q} \leq 6000$ W/m²		$9000 \leq \dot{q} \leq 11000$ W/m²		$\overline{(\Delta p / \Delta p_{pt})}(x_m)$
	mean value $\overline{(\alpha/\alpha_{pt})}(x_m)$	maximum value $(\alpha/\alpha_{pt})_{max}(x_m)$	mean value $\overline{(\alpha/\alpha_{pt})}(x_m)$	maximum value $(\alpha/\alpha_{pt})_{max}(x_m)$	
SP	1.09-1.34	1.58	0.83-1.2	1.64	2,1-2,5
WP	1.05-1.12	1.31	1.14-1.34	1.60	3,4-4,5
Fin	0.77-1.11	1.32	0.71-1.22	1.27	1,5-1,9

4. Summary

The effectiveness of heat transfer enhancement achieved by using the analysed inserts may be assessed on the basis of the ratio of the transferred heat flux $\dot{Q}$ to the refrigerant discharge power $(\dot{V}\Delta p)$. In the case under consideration, it was assumed that the volumetric flow rate of the refrigerant corresponded to the saturation conditions for pressure p_{Rout} ($\dot{V} = \dot{V}''(p_{Rout})$). For greater vapour quality values, inserts that generate low flow resistances have a better thermal power coefficient referred to discharge power ($E = \dot{Q}/(\dot{V}\Delta p)$), which stems from an increase in the refrigerant flow velocity. Therefore, despite a moderate increase in heat transfer coefficients for a Fin insert as compared to an SP insert, low flow resistances call for the use of a Fin insert. For low vapour quality values, i.e. $x_m < 0.5$, WP inserts have a better ratio of thermal power to discharge power than Fin and SP inserts. The WP inserts with high flow resistances may be used in particular with zeotropic refrigerants with a high temperature glide and with low mass flux values $\dot{G} < 100$ kg/(m²s). The Fin and SP inserts may be used in the whole vapour quality range.

References

[1] Regulation (EU) No. 517/2014 of the European Parliament and of the Council

[2] Ribatski G., Thome J.R., *Nucleate boiling heat transfer of R134a on enhanced tubes*, Applied Thermal Engineering, Vol. 26, 2006, 1018–1031.

[3] Ding G., Hu H., Huang X., Deng B., Gao Y., *Experimental investigation and correlation oft two-phase frictional pressure drop of R410A-oil mixture flow boiling in a 5mm micro-fin tube*, International Journal of Refrigeration, Vol. 32, 2009, 150–161.

[4] Bandarra-Filho E.P., Barbieri P.E.L., *Flow boiling performance in horizontal microfinned copper tubes with the same geometric characteristics*, Experimental Thermal and Fluid Science, Vol. 35, 2011, 832–840.

[5] Kabelac S., de Buhr H.J., *Flow boiling of ammonia in a plain and low finned horizontal tube*, International Journal of Refrigeration, Vol. 24, 2001, 41–50.

[6] Padovan A., Del Col D., Rossetto L., *Experimental study on own boiling of R134a and R410A in a horizontal micro n tube at high saturation tubes*, Applied Thermal Engineering, Vol.31, 2011, 3814–3826 .

[7] Sami S.M., Desjardnis D.E., *Prediction of convective boiling characteristics of alternatives to R502 inside air/refrigerant enhanced surface tubing*, Applied Thermal Engineering, Vol. 20, 2000, 579–593 .

[8] Targański W., Ciesliński J., *Evaporation of 407C/oil mixtures inside corrugated and micro-fin tubes*, Applied Thermal Engineering, Vol. 27, 2007, 2226–2232.

[9] Kim N.H., Lee E.J., Byun H.W., *Evaporation heat transfer and pressure drop of R410A in flattened plain tubes having different aspect ratios*, International Journal of Refrigeration, Vol. 36, 2013, 363–374.

[10] Akhavan-Behabadi M.A., Kumar R., Mohammadpour A., Jamali-Ashatini M., *Effect of twisted tape insert on heat transfer and pressure drop in horizontal evaporators for the flow of R134a*, International Journal of Refrigeration, Vol. 32, 2009, 922–930.

[11] Mogaji T.S., Kanizawa F.T., Filho E.P.B., Ribatski G., *Experimental study of the effect of twisted-tape inserts on flow boiling heat transfer enhancement and pressure drop penalty*, International Journal of Refrigeration, Vol. 36, 2013, 504–515.

[12] Yun R., Hwang J-S., Chung J.T., Kim Y., *Flow boiling heat transfer characteristics of nitrogen in plain and wire coil inserted tubes*, International Journal of Heat and Mass Transfer, Vol. 50, 2007, 2339–2345.

[13] Niezgoda-Żelasko B, Żelasko J., *Free and forced convection on the outer surface of vertical longitudinally finned tubes*, Experimental Thermal And Fluid Science, Vol. 57, 2014, 145–156.

[14] Lemmon E.W., Huber M.L., McLinden M.O., *NIST Standard Reference Database 23: Reference Fluid Thermodynamic and Transport Properties Database REFPROP*, Gaithersburg 2010.

[15] Thome J.R., *Engineering data book III,* Wolverine Tube, Inc. 2004–2010.